Electrochemical capacitive performance of intact anaerobic granular sludge-based 3D bioanode

Zhao, Nannan; Su, Yanyan; Angelidaki, Irini; Zhang, Yifeng

Published in:
Journal of Power Sources

Link to article, DOI:
10.1016/j.jpowsour.2020.228399

Publication date:
2020

Document Version
Peer reviewed version

Elsevier Editorial System(tm) for Journal of Power Sources

Manuscript Draft

Manuscript Number: POWER-D-20-01891R1

Title: Electrochemical capacitive performance of intact anaerobic granular sludge-based 3D bioanode

Article Type: Research Paper

Keywords: Supercapacitor; Anaerobic granular sludge; Exoelectrogens; Bioanode; Energy storage; Capacity

Corresponding Author: Dr. Yifeng Zhang,

Corresponding Author's Institution: Technical University of Denmark

First Author: Nannan Zhao

Order of Authors: Nannan Zhao; Yanyan Su; Irini Angelidaki; Yifeng Zhang

Abstract: In search of clean, renewable and efficient supercapacitors, electrogenic microbes have been shown as a promising alternative biomaterial for energy storage. In this study, intact methanogenic granular sludge with a unique spherical structure consisting of dense microbial community was for the first time demonstrated as an efficient exoelectrogenic bioanode of supercapacitor for energy storage. The maximum capacity of 1542.7 ± 203.2 mC is achieved by the exoelectrogenic granular sludge (EGS, 20 grams) based bioanode at the anodic potential of +0.2 V VS Ag/AgCl and with 5 minutes charge and 10 minutes discharge cycle. The capacitance of the EGS bioanode is 2-3 orders of magnitude higher compared to methanogenic one. The amount of EGS is found critical to the system capacitance. The electrochemical behavior of single EGS suggests the cytochromes, which had close contact with the flat graphite or gold wire electrode, plays an important role as an electron conduit between the electrochemical granule and the electrodes. The superior electron storage capacity of the EGS is probably related to its potential double-layer structure and enrichment of exoelectrogenic bacteria having conductive c-type cytochromes. This proof-of-concept study offers insights into the future development of bio-based sustainable, low cost and environmental-friendly supercapacitor.

Graphical Abstract

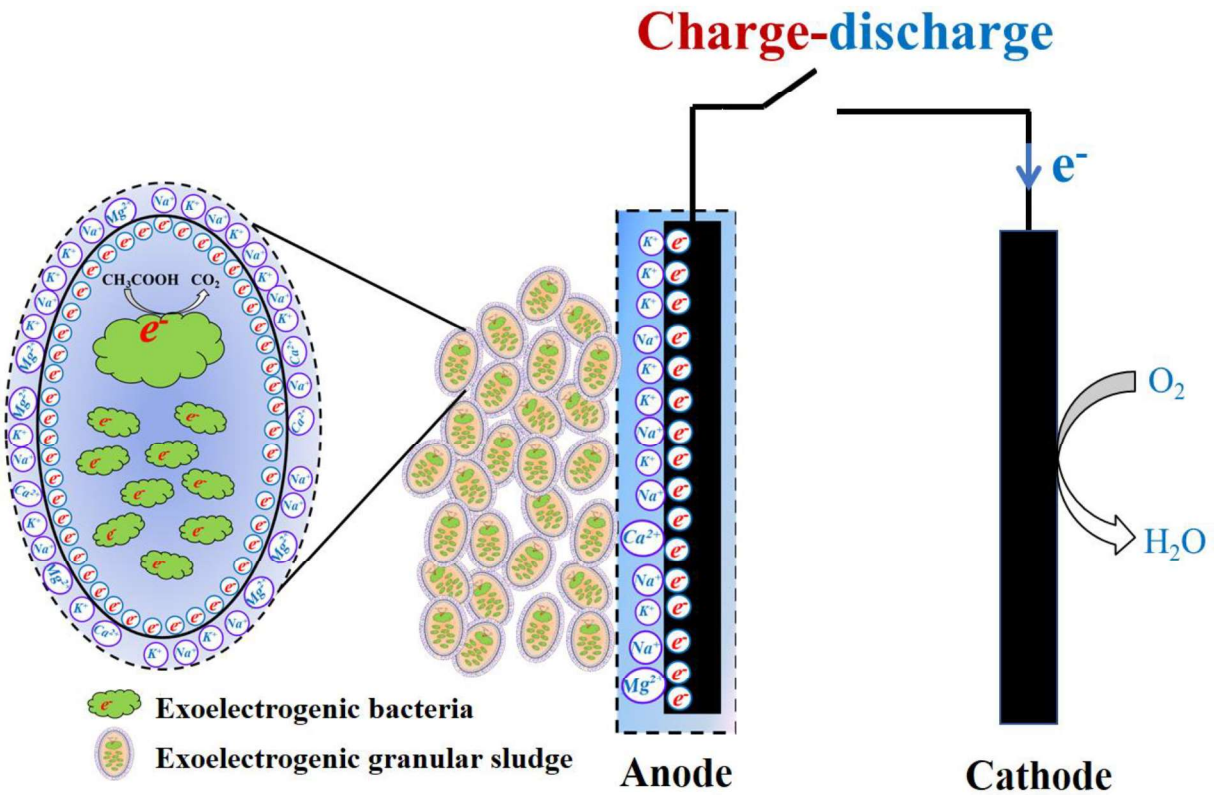

Highlights

- Electrogenic granular sludge as a biocapacitor for electron storage.
- Capacitance of electrogenic granular sludge outperformed methanogenic one.
- Capacitance increased with anode potential and amounts of granules.
- Single granule was in close contact with electrode via cytochromes.
- Cytochromes mainly contributed to the capacitance of such biocapacitor.

Electrochemical capacitive performance of intact anaerobic granular sludge-based 3D bioanode

Nannan Zhao[a], *Yanyan Su*[b], *Irini Angelidaki*[a], *Yifeng Zhang*[a*]

[a] Department of Environmental Engineering, Technical University of Denmark, DK-2800 Lyngby, Denmark.

[b] Carlsberg Research Laboratory, Bjerregaardsvej 5, 2500 Valby, Denmark

[*]Corresponding author, Tel.: +45 45251410; fax: +45 45932850.
E-mail address: yifz@env.dtu.dk; yifzmfc@gmail.com (Yifeng Zhang)

Abstract

In search of clean, renewable and efficient supercapacitors, electrogenic microbes have been shown as a promising alternative biomaterial for energy storage. In this study, intact methanogenic granular sludge with a unique spherical structure consisting of dense microbial community was for the first time demonstrated as an efficient exoelectrogenic bioanode of supercapacitor for energy storage. The maximum capacity of 1542.7 ± 203.2 mC is achieved by the exoelectrogenic granular sludge (EGS, 20 grams) based bioanode at the anodic potential of +0.2 V VS Ag/AgCl and with 5 minutes charge and 10 minutes discharge cycle. The capacitance of the EGS bioanode is 2-3 orders of magnitude higher compared to methanogenic one. The amount of EGS is found critical to the system capacitance. The electrochemical behavior of single EGS suggests the cytochromes, which had close contact with the flat graphite or gold wire electrode, plays an important role as an electron conduit between the electrochemical granule and the electrodes. The superior electron storage capacity of the EGS is probably related to its potential double-layer structure and enrichment of exoelectrogenic bacteria having conductive c-type cytochromes. This proof-of-concept study offers insights into the future development of bio-based sustainable, low cost and environmental-friendly supercapacitor.

Keywords: Supercapacitor; Anaerobic granular sludge; Exoelectrogens; Bioanode; Energy storage; Capacity

1. Introduction

The increasing demand of energy globally along with the wish for carbon-neutral societies have created urgent needs on both sustainable energy conversion and storage technologies [1-4]. Among the available technologies, electrochemical capacitors (EC) [5], which reply on the materials with large surface area and porous boundary layer, are emerging as effective and practical devices to preserve electrical energy [6-8]. Nevertheless, the conventional materials used in EC are mainly carbon or metal oxide particles, which are relatively expensive and are not renewable.

Recently, exoelectrogens, a specific group of bacteria that can oxidize organic matter and transfer released electrons extracellularly to the electrode, provide a promising way to harvest electrical energy or other valuable products from waste streams [2, 9]. In addition to electricity generation, the electroactive biofilm formed by exoelectrogenic bacteria growing on granular activated carbon has been demonstrated as a promising biological material to develop biocapacitor (i.e., supercapacitor) for charge storage [10, 11]. Such biocapacitor mainly utilizes the redox cofactors of exoelectrogens (e.g., c-type cytochromes) and electrical double layer of granular activated carbon to store electrons [12, 13]. Compared to conventional EC, the biocapacitor has tremendous advantages in terms of cost, renewability and sustainability [12]. Furthermore, the biocapacitor integrates waste-to-electricity conversion and charge storage into a single system, which may greatly simplify the energy system and reduce the capital and operating costs. The discovery of such unique property of electroactive biofilm and the invention of biocapacitor opens up a new door for the development of sustainable energy storage devices. However, the development of such a novel energy storage system is still

in its infancy. Among others, the development of efficient and thick biofilm and further reduction of material costs (i.e., to replace granular activated carbon) are the two key issues to be addressed.

In this context, methane-producing microbial consortia as granular sludge have come to attention as a promising biological capacitive material due to their outstanding characteristics. Granular sludge consisting of microbial associations that are well kept together by extracellular polymers is typically used in upflow sludge blanket reactors [14]. Firstly, anaerobic granular sludge has a unique 3D porous structure, which is quite similar to the typical conductive material (e.g., granular activated carbon). This specific structure will help granular sludge to build up a double layer for the storage of electrical charges. Secondly, innate granular sludge could be turned into conductive (exoelectrogenic) by enriching electroactive microbes. It has been reported that the microbial aggregates were conductive as a result of the enrichment of exoelectrogens in syntrophic cultures [15, 16]. Thirdly, granular sludge has quite dense microbial communities compared to 2D thin biofilm. Fourthly, granular sludge as biological material is green, cheap and renewable. For instance, compared to granular activated carbon covered by biofilm, granular sludge will greatly reduce the electrode material costs owing to the spherical structure and innate massive microbes. The commercial prices for granular sludge and activated carbon are 0.22 Euro and 55 Euro per kg. With this novel biomaterial, charging in biocapacitor could be achieved via oxidation of electron carrier by granular sludge followed by storage of released electrons in proteins and double layer, while the discharging could be realized through connecting the bioanode and cathode to external circuit.

In this study, an exoelectrogenic granular sludge (EGS) was acclimatized from intact methanogenic granular sludge and explored as an alternative bioanode material of biocapacitor for energy storage. The EGS-based bioanode was exhibiting superior charge-storage capability (70 times higher) compared to that of methanogenic one. The maximum charge storage of 1542.7 ± 203.2 mC was achieved with 5 minutes charge and 10 minutes discharge cycle at the anodic potential of +0.2 V vs Ag/AgCl. Additionally, electrochemical characterization of single granule demonstrated the unique electrochemical activity of the outer layer of single granule contacted with the electrode, which may server as electric conduit between microbes and electrode for long-range extracellular electron transfer and, contribute to the formation of the double layer. Microbial dynamics under chronoamperometry did reveal the enrichment of exoelectrogenic bacteria. Based on these findings, a potential charge-storage mechanism was also proposed.

2. Material and methods

Anaerobic granular sludge. 100 g granular sludge were collected from a mesophilic up-flow anaerobic sludge blanket reactor fed with potato wastewater (Colsen, Netherland), and maintained at 4 °C under anaerobic conditions (flashed with N_2 for 30 minutes). Before starting experiments, the granular sludge was kept at room temperature (25 ± 2 °C) for 2 hours, for reviving the activity of microbes. To distinguish, the original granular sludge was denoted as methanogenic granular sludge and the electrochemically acclimated granular sludge was denoted as exoelectrogenic granular sludge (EGS).

Bio-capacitor set-up and single granule reactor design. Two identical bio-capacitors, denoted as biocapacitor1 and biocapacitor2, were constructed. Each bio-capacitor was composed of 20 g granular sludge embedded in a two-neck glass flask (500 ml, WO Schmidt, Germany), as shown in Figure S1. A carbon brush used as anode electrode (working electrode), which provided a good contact with granule sludge. All the experiments were carried out under three-electrode configuration controlled by a multi-channel potentiostat (Metrohm Autolab, Germany). The counter electrode consisted of a stainless-steel mesh with a surface area of 0.1 m^2 (Ludwig Ohlendorf KG, Germany). An Ag/AgCl (sat. KCl) electrode (Sensortechnik Meinsberf, Germany) served as the reference electrode. All the potentials reported in this study are versus Ag/AgCl (+0.197 V vs standard hydrogen electrode). The counter electrode and reference electrode were placed close to the working electrode (carbon brush) to diminish the electrolyte effect (iR drop). The medium was synthetic wastewater prepared according to Kim et al [17], supplemented with sodium acetate (10 mM) and vitamin and trace elements [18]. To fully immense all the three electrodes and granule sludge, 350 ml media (purged with pure N_2 for 30 minutes before use) were carefully added into the anode chamber. After media replacement, the whole device was sparged with pure N_2 for another 30 minutes to ensure strict anaerobic environment during experiments. The temperature was maintained at room temperature (25 ± 2 °C). During the conversion of the granular sludge from methanogenic into exoelectrogenic condition, chronoamperometry (CA) namely potential control, was conducted with an anodic potential of +0.2 V to form EGS. Controlling anodic potential was demonstrated as the optimal strategy to covert the granule from methanogenic to exoelectrogenic [19].

To characterize the electrochemical behavior of a single granule, two sets of different reactors were installed. Both sets of reactors were based on a four-neck glass flask (20 ml). In the experiment of single granule sludge growing on a flat electrode, polished flat graphite with a surface area of 0.2 cm^2 was used as the working electrode. In the experiment of single granule sludge wrapped with gold wire, gold wire (0.1 mm diameter, approximately 5 cm length) was wrapped around the granule sludge surface to ensure a good contact, serving as a working electrode. For both reactors, the working electrode and reference electrode were graphite rod and Ag/AgCl electrode. The reactors were fed with 10 ml sodium acetate medium (10 mM) as described above. The reactors were purged with pure N_2 for 30 minutes before testing. All experiments were conducted in duplicate.

Charge-discharge experiments. To evaluate the capacitive property of the biocapacitor, charge-discharge tests were conducted. A single cycle included a charge period (open-circuit mode) and a discharge period (reactor operation at a setting anodic potential). The biocapacitor was fully discharged for 1 hour before starting each cycle. For all charge-discharge experiments, ten consecutive cycles were performed, on which all the calculations were based. In the experiment of multi-parameter effects, three different anodic potentials (-0.2 V, 0 V, +0.2 V) were first applied to the discharge period, respectively. Different charge-discharge cycles including 5 min - 10 min, 10 min - 5 min, 10 min - 30 min, and 20 min - 60 min were chosen as described in Table 1.

Electrochemical measurements. All the electrochemical characterizations were carried out by a multi-channel potentiostat (Metrohm Autolab, Germany). After

reproducible current generation during CA at 0.2 V, polarization curves were performed to determine current response as a function of varied anode potential. The anode potential was varied from -0.5 to +0.2 V, with the step of 0.05 V. For each anode potential, it was kept for at least 20 minutes until the current output was stable. The average current outputs for polarization curves were taken from the last 5 minutes at each potential. Cyclic voltammetry (CV) was performed whenever the current achieved the maximum value (turnover CV) and when the current declined to a minimum value (non- turnover CV). Anode potential was swept from -0.5 to 0.2 V versus Ag/AgCl at a scan rate of 1 mV s^{-1}.

Microscopy. Scanning electron microscope [20] (FEI Quanta 200 ESEM FEG, Germany) test was performed to characterize the morphology of granule sludge after acclimation experiment using CA. Granule sludge was prepared by fixing with 4% formaldehyde overnight at 4 °C and dehydrating with successive passage through gradient 25%, 50%, 75%, 95% and 100% ethanol and subsequently freeze dried. The prepared granule sludge was coated by nano-gold (Quorum sputter coater, UK) and observed with the SEM.

For the Raman microscopic analysis, single granule sludge was gently removed from the anode chamber, and transferred immediately to a sterilized glass slide. The Raman measurements were performed using the Renishaw RAMAN spectrometer InVia REFLEX. To enable an effective resonant excitation in the cytochromes, the laser light of 532 nm was chosen. The excitation energy was set below and each spectrum was recorded at the corresponding site of the sample (as explained earlier). For the

measurement of different sites, the angle of the microscopic lens was modified to fit the requirements. Though only one single spectrum was displayed as representative at each sample site, in some cases, up to five similar spectra were taken to improve the resolution. About the acquisition time, each operational parameter was displayed in each Raman spectra caption. Baseline subtraction was performed for all the spectra in the software Renishaw WiRE.

Capacitive charge and charge recovery calculations. Theoretical charge-discharge was displayed in Figure S2. The total cumulative charge Q_{cumm} was calculated by integral of current and time all along the whole period, as demonstrated by equation 1, where Q_{cumm} is the sum of capacitive Q_{cap}, Q_{st}, Q_{cap} refers to the capacitive charge contributed by the capacitive current, and Q_{st} refers to the stable charge contributed by the faradic current. t_1 is the whole period time including charge and discharge, and I_i is the measured current that flowed from anode to cathode. The cumulative total charge was calculated to get further sights into the storage capacity and stability (equation 4).

$$Q_{cumm} = \int_{t0}^{t2} I_i dt \quad \text{Eq (1)}$$

$$Q_{st} = i_s t_d \quad \text{Eq (2)}$$

$$t_d = t_2 - t_1 \quad \text{Eq (3)}$$

$$Q_{cap} = Q_{cumm} - Q_{st} \quad \text{Eq (4)}$$

$$\eta_{rec} = \frac{Q_{cumm}}{nQ_{st}} \quad \text{Eq (5)}$$

The expected charge Q_{exp} was calculated as equation 2, where i_s is the steady state current when the cell achieved stable during discharge period, and t_d is the discharge time (equation 3).

The relative charge recovery (η_{rec}), as an indicator of energy stored in bioanode, was calculated according to equation 5 based on the data obtained from 10 consecutive cycles. n was the number of charge and discharge cycles.

There are three conditions the charge recovery could achieve: (1) when charge recovery is larger than 1, the measured total charge is higher than the expected charge. (2) when charge recovery is equal to 1, the measured charge is equal to the expected charge. (3) when charge recovery is smaller than 1, the measured charge is lower than the expected charge.

Microbial community dynamics under chronoamperometry. The microbial community was analyzed by 16s rRNA sequencing. For the single granule experiment, it's impossible to analyze the microbial community dynamics before and after the CA at one time. Therefore, we designed a separate experiment to decipher the change of microbial composition. Similar installation was performed as following. 80 g of granule sludge was placed in the anode chamber, surrounded by a carbon brush. The reference electrode Ag/AgCl was placed close to the anode. The counter electrode was a titanium woven wire mesh (4×4 cm, 0.15 mm aperture, William Gregor Limited, London) coated with 0.5 mg cm^{-2} Pt. The same acetate-rich medium was fed to the reactor. A similar CA procedure was performed to turn the methanogenic granular sludge to exoelectrogenic. The anodic potential was controlled at +0.02 V, and the current response was recorded by

a potentiosat (Ivium-n-Stat, Ivium Technologies, Eindhoven, The Netherlands). The formation of EGS was recognized by a significant increase in current and later confirmed by 16s rRNA.

EGS was collected to analyze the microbial community composition, in comparison to the fresh methanogenic granular sludge. PowerSoil DNA Isolation Kit (MoBio PowerSoil, Carlsbad, CA, USA) was used to extract the total DNA. Universal primers 515F/806R were used to amplify the total genomic DNA on the V4 hypervariable region of 16S rRNA gene, and the amplicons were sequenced using Illumina MiSeq desktop sequencer (Ramaciotti Centre for Genomics, Kensington, Australia). Raw data were deposited in the Sequence Read Archive database (https://www.ncbi.nlm.nih.gov/sra) under the project number PRJNA451128.

CLC Workbench software (V.8.0.2, QIAGEN) equipped with the Microbial genomics module plugin was used for OUT clustering and taxonomy identification as previously described [21]. The taxonomical assignments of the selected interesting OTUs (relative abundance over 0.1%) were conducted including a manual comparison of CLC results with 16S ribosomal RNA sequences (Bacteria and Archaea) database at the National Center for Biotechnology Information (NCBI) by using BLAST [21].

3. Results and discussion

3.1. EGS and charge-storage capability

Scanning electron microscopy (SEM) analysis was first employed to visualize the morphology of EGS [20]. The EGS had a spherical rough surface with porous structure

(Figure S3), together with the enrichment of exoelectrogenic microbes from out and inside, it would allow a potential electrical double layer effect when immersed in an electrolyte [15, 22]. Besides, the big surface area of granular sludge would be beneficial for the enrichment of exoelectrogens [23]. The mechanical strength of the granular structure offered a robust supportive skeleton for microbes to withstand the environmental changes in the surroundings (such as shaking or moving) compared to other conventional exoelectrogenic biofilms [14, 24]. Besides, rod-shape microorganisms - a shape of microorganisms commonly found in electroactive biofilm [25, 26] - were observed in high-resolution images (Figure S3b). There were multi-channels with approx. 1 μm diameter which were probably used for gas transportation inside of EGS (Figure S3c and S3d) [27]. Overall, EGS had unique physical properties which may allow it to be an ideal biological capacitive material for storage of electric charge.

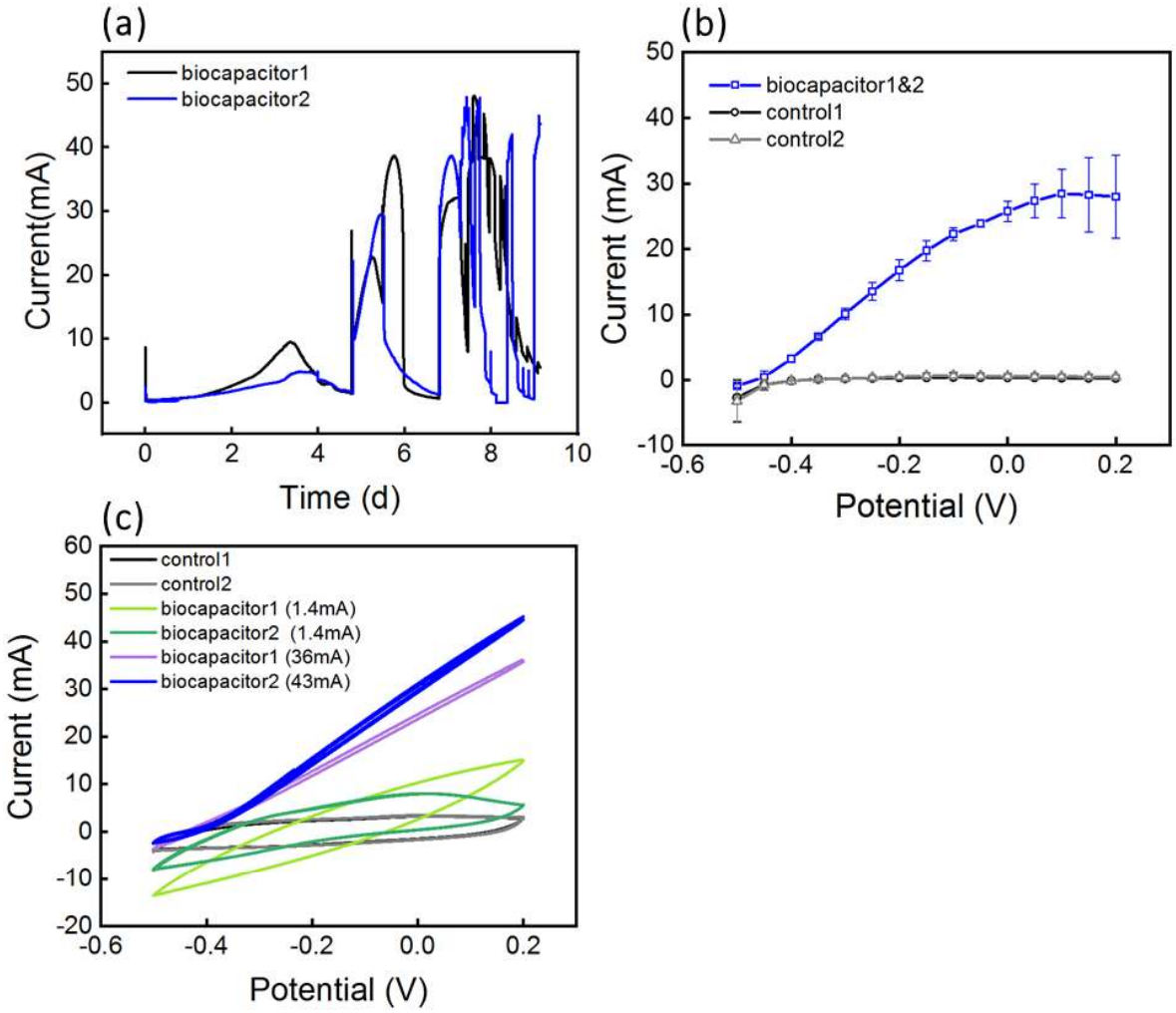

Figure 1. Electrochemical characterization profiles of biocapacitor with different bioanodes. (a) Chronoamperometric plot of duplicate EGS-based biocapacitor systems during enrichment; (b) Polarization curves of the systems with EGS anode, abiotic anode (Control 1) and methanogenic granular sludge-based anode (Control 2); (c) Cyclic voltammogram of different bioanodes. 10 mM of acetate was used as substrate, for all the above tests.

To transform methanogenic into electrogenic granules, chronoamperometry (CA) was performed to enrich the exoelectrogens in the granular sludge. The working electrode

potential was set as +0.2 V, which was previously reported to be energetically favorable for the growth of exoelectrogens [28]. The CA profile (Figure 1a) illustrates the successful enrichment of exoelectrogens after 7 days of operation. Once reproducible high biocurrent (around 40 mA) was obtained after approx. 8 days, the electrocatalytic activity of the EGS bioanode was characterized by conducting a polarization curve test. As depicted in Figure 1b, maximum biocurrent of 28.4 mA was generated by the EGS bioanode at the anodic potential of 0.1 V, while the current derived from the abiotic anode (control1) or methanogenic granular sludge bioanode (control2) was negligible. The results suggest the biocurrent was mainly derived from bioelectrocatalytic activity and was dependent on the anodic potential. Subsequently, cyclic voltammetry (CV) was exploited to obtain a straightforward view of the bioelectrocatalytic activity of EGS-based bioanode. As shown in Figure 1c, CV profiles of both biocapacitors showed a similar trend. The CV curves of the abiotic anode, methanogenic granular sludge anode and inactivated EGS anodes (low current response of 1.4 mA during CA period) all showed insignificant exoelectrogenic signal. Differently, the CV profile recorded with the enriched EGS exhibited an enhanced current signal at high potential, which was attributed to the electroactivity of exoelectrogens [29, 30]. Slightly different from the typical sigmoidal shape, the current signal didn't reach a plateau value when the anodic potential increased above 0 V. The continuing increasing current at high anodic potential suggested either a diffusion issue or limited electron transfer without the presence of extracellular redox mediators [31]. The above results demonstrated that the EGS-based bioanode was successfully transformed from methanogenic to exoelectrogenic.

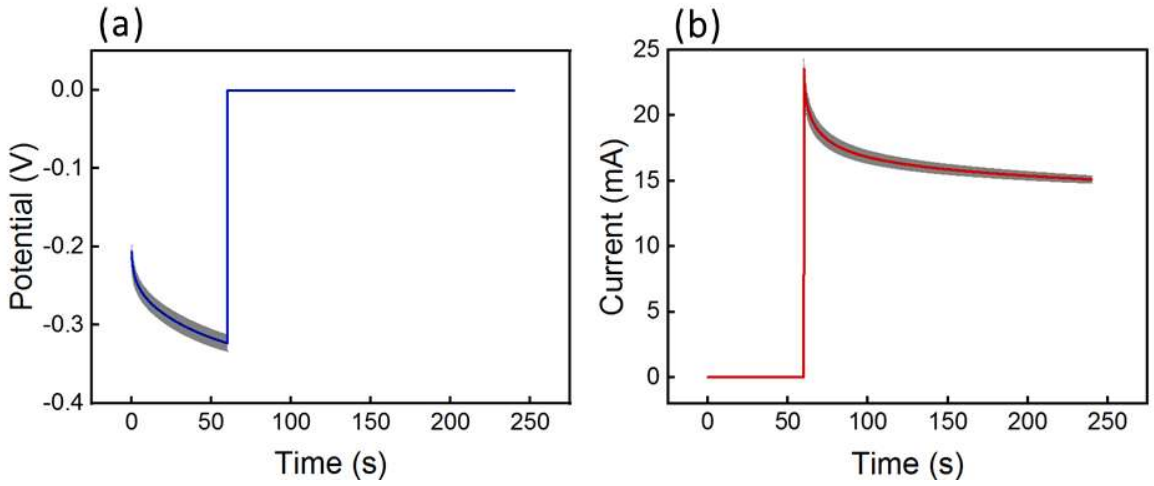

Figure 2. Typical charge-discharge test at 0 V. (a) Anodic potential change and (b) current response during cycles of 60 s charge and 180 s discharge period (n=10).

As previously reported, during the electron transfer process between electroactive microorganisms and electrode, specific groups of redox cofactors (i.e. cytochromes) can accumulate charges temporarily [32, 33], which is one of the identified mechanisms of biocapacitors. Considering the porous structure of granular sludge which might be able to harbor dense microbial communities and the potential enrichment of electroactive bacteria after the CA approach, the EGS bioanode could have the potential to store electric charge. To evaluate the feasibility, a cycle test, including one open circuit mode and one period with control of anodic potential at 0 V, was applied [10]. The biocapacitor was charged when it was in open circuit, and discharged when the anodic potential was controlled. The anodic potential of 0 V was chosen, because the current response reached a plateau with small standard deviation values at this potential (according to the polarization curve shown in Figure 1b). The representative profile of charge-discharge cycles is given in Figure 2.

In the open circuit (charging), the anodic potential showed an immediate decrease (0.12 ± 0.01 V), which was mainly due to the negatively charged state of the EGS based bioanode as a result of the continuing metabolic oxidation of the substrate. After switching it back to the closed-circuit (discharging), the cell showed a quite typical capacitive current signal (Figure 2b). Thereafter, the current decreased towards a stable value, which was usually regarded as the faradic current generated by the metabolic oxidation of redox cofactors at the electrode. From mathematic calculation based on the integral equation of current with time, the cumulative Q, stable Q, and capacitive Q were obtained (see Methods section). Capacitive Q is an important indicator to evaluate the performance of a capacitor. The higher Q value, the higher the capacity would be. Among ten consecutive cycles, the cells had a peak current of 23.54 ± 0.74 mA during the first 100 seconds, and then it reached a stable value of 15.11 ± 0.29 mA. The capacitive Q was 211.3 ± 24.06 mC. When compared to the capacitive Q of the biocapacitor with methanogenic granular sludge (-3.8 ± 6.1 mC at 0 V anode potential, Figure S4), the results demonstrate the superior capacitive performance of the biocapacitor with EGS (211.3 ± 24.06 mC at 0 V anode potential). It has been demonstrated that the phosphor-lipid bilayer structure of cells, c-type cytochromes and nanowires in/on cell membrane enabled electroactive bacteria working as a bioanode material of biocapacitor [33, 34]. Thus, the superior biological capacitance of the EGS bioanode was probably due to the enrichment of exoelectrogenic bacteria and the associated cytochromes. To the best of our knowledge, this is the first study that demonstrated the feasibility of EGS-based bioanode as the capacitive material of biocapacitor.

3.2. Multi-parameter effects on the capacitive performance

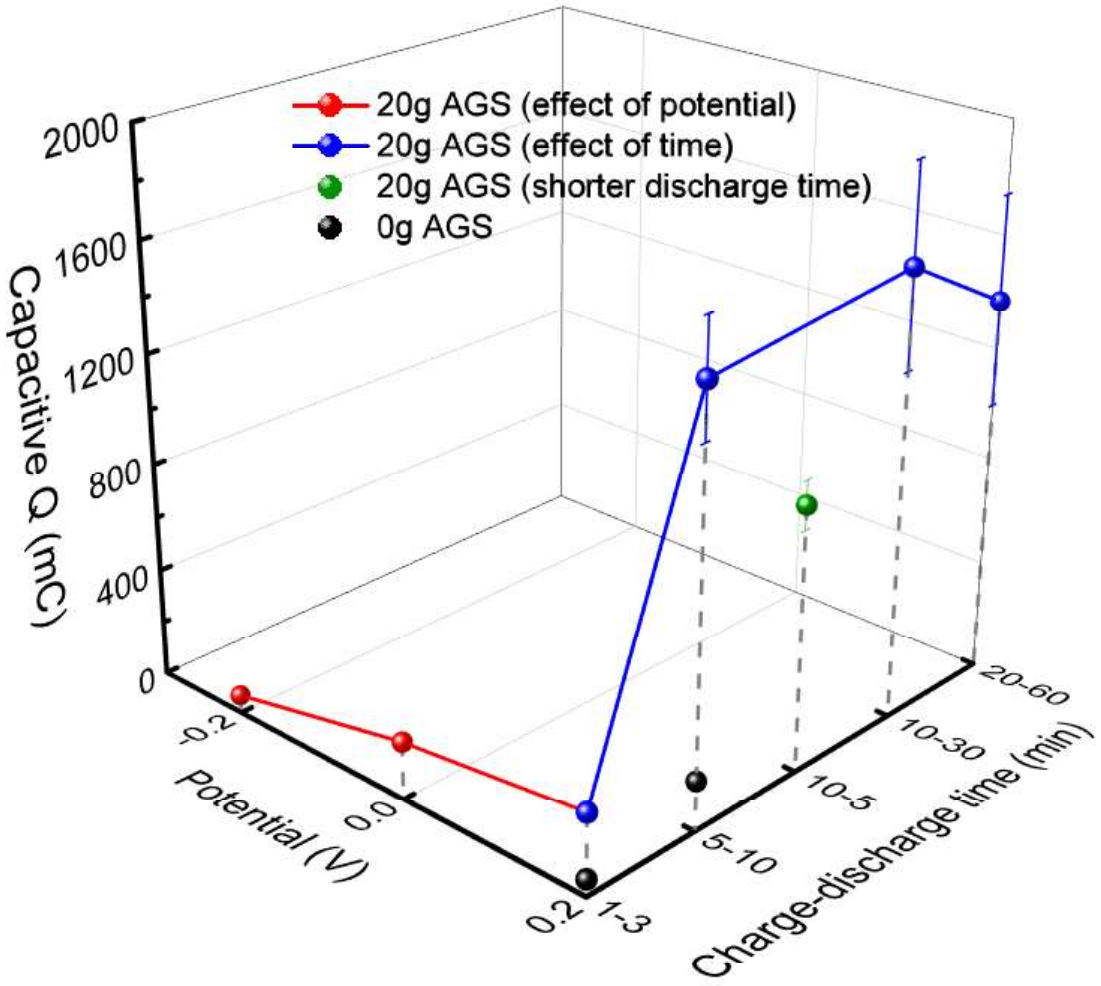

Figure 3. Capacitive Q at multi-parameter conditions. Red circles represent effect at different potentials with 1 min charge and 3 min discharge cycle; Blue circles represent effect of charge-discharge times; Specially, green circles refer to the capacitive Q when the discharge time was shorter than charge time; Black circles represent the control (0 g EGS) with 1-3 min and 5-10 min charge-discharge time, respectively. Unless stated otherwise, 20 g EGS were used and anodic potential was controlled at 0.2 V. All the error bars are standard deviations for n = 10 measurements.

The anode potential has been reported as an effective strategy to suppress methanogens and enrich electroactive bacteria [35]. Thus, it may affect the capacitive performance of EGS bioanode. To verify this hypothesis, the performance of EGS bioanode at three different anodic potentials including -0.2, 0 and 0.2 V was investigated. It was found that capacitive Q increased with increasing anodic potential and reached to 296.3 ± 16.6 mC at the anodic potential of 0.2 V (Figure 3). Furthermore, the relative charge recovery, defined as the ratio of capacitive current and faradic current, was stable at around 1.08 with the tested anode potentials (Table 1). The increase of protein (i.e. cytochromes associated with electron storage) or exoelectrogenic activity at more positive potential [36, 37] could contribute to the increase of capacitive Q when the anodic potential increased from -0.2 to 0.2 V. Besides, the relative charge recovery didn't change with anodic potential when it increased from 0 to 0.2 V (Table 1), which was probably because the faradic current increased along with capacitive current at higher anodic potential. Based on the above, the anodic potential of 0.2 V was chosen for the following tests.

Table 1. Relative charge recovery (ηrec) under different operating conditions during 10 consecutive charge-discharge experiments. When the value is over 1, the measured total charge was higher than the expected charge. (1 min - 3 min means charge for 1 minute, discharge for 3 minutes.)

20 g EGS			20 g EGS	0 g EGS
-0.2 V	0 V	0.2 V	0.2 V	0.2 V

	1 - 3 min			5 - 10 min	10 - 5 min	10 - 30 min	20 - 60 min	1 - 3 min	5 - 10 min
ηrec	1.04	1.08	1.08	1.22	1.28	1.34	1.36	1.01	1.01
	±0.00	±0.01	±0.01	±0.01	±0.02	±0.02	±0.03	±0.00	±0.00

Charge and discharge time is a representative indicator to evaluate a capacitor [38]. Thus, the effect of different charge and discharge time on the capacitance of the EGS bioanode was investigated. Notably, as shown in Figure 3 capacitive Q was dramatically improved from 296.3 ± 16.6 to 1542.7 ± 203.2 mC when the charge-discharge time was increased from 1 min - 3 min to 5 min - 10 min. When the charge and discharge time was further increased (i.e. 10 min - 30 min, and 20 min - 60 min), no further significant improvement of the capacitive Q was observed. The capacitive Q tended to maintain stable around 1600 mC. The increasing standard deviation at 10 min - 30 min and 20 min - 60 min indicated the low stability of biocapacitor when the time was prolonged. A similar trend was observed for relative charge recovery as well. Moreover, when the discharge time was shorter than the charge time (10 min - 5 min), the capacitive Q showed a decreasing trend compared to the capacitive Q at 10 min - 30 min (Table 1). It means, that the discharge time needs to be longer than charge time, to have adequate time to capture all the capacitive Q. Trading-off the stability and capacitive Q, the optimal charge-discharge time was selected as 5 min – 10 min, and the corresponding capacitive Q was 1542.7 ± 203.2 mC. It has been reported that a single activated carbon granule based bioanode accumulated 860 mC electrons in a 1 min charging and 3 min discharging period [11]. In

our study, 20 g EGS stored 1542.7 ± 203.2 mC. With comparable or even higher capacitance, the EGS bioanode holds unique merits of cheap, green, and renewable. It is expected that the capacitance of the EGS could be further improved in the future by addressing the following challenges. Firstly, good contact between the granules should be maintained to reduce the internal resistance when high amounts of granules are put together in the anode. It could be tackled by using current collectors [39]. Secondly, EGS, as a biomaterial, its conductivity should be improved to be comparable to the abiotic materials such as carbon granule. It could be realized by doping inexpensive catalysts into the EGS during the granulation period. Furthermore, reliable cycling durability was proved after a long-term operation (10 consecutive cycles), which was another merit of EGS bioanode.

To identify the effect of EGS quantities on biocapacitor performance, different amounts of EGS were removed from the anode chamber. The capacitive Q and relative charge recovery were calculated based on the 10 consecutive cycle tests. As depicted in Figure 3, capacitive Q and the relative charge recovery notably decreased when EGS were removed, regardless of charge-discharge time. In 5 min charge and 10 min discharge cycle, the capacitive Q and relative charge recovery were decreased dramatically from 1542.7 ± 203.2 mC and 1.22 ± 0.01 to 184.3 ± 9.3 mC and 1.01 ± 0.00, respectively. Similarly, in 1 min charge and 3 min discharge cycle, the capacitive Q and relative charge recovery decreased from 296.3 ± 16.6 mC and 1.08 ± 0.01 to 62.1 ± 1.2 mC and 1.01 ± 0.00, respectively. The results above implied a strong correlation between EGS quantity and biocapacitor performance. It could be explained by the presence of exoelectrogens. Generally, the higher content of exoelectrogens in granular sludge, the more capacitive material (i.e., electron shuttles, c-type cytochromes and/or nanowires) may be

available [40], resulting in higher capacitance of the biocapacitor. Additionally, the special granular structure including the channels and pores on the granule surface may create the electrical double layer [41]. In this context, when EGS were totally removed, not only exoelectrogens and the associated redox cofactors may decrease, but also the electrical double layer would disappear.

3.3. Electrochemical behavior of single EGS

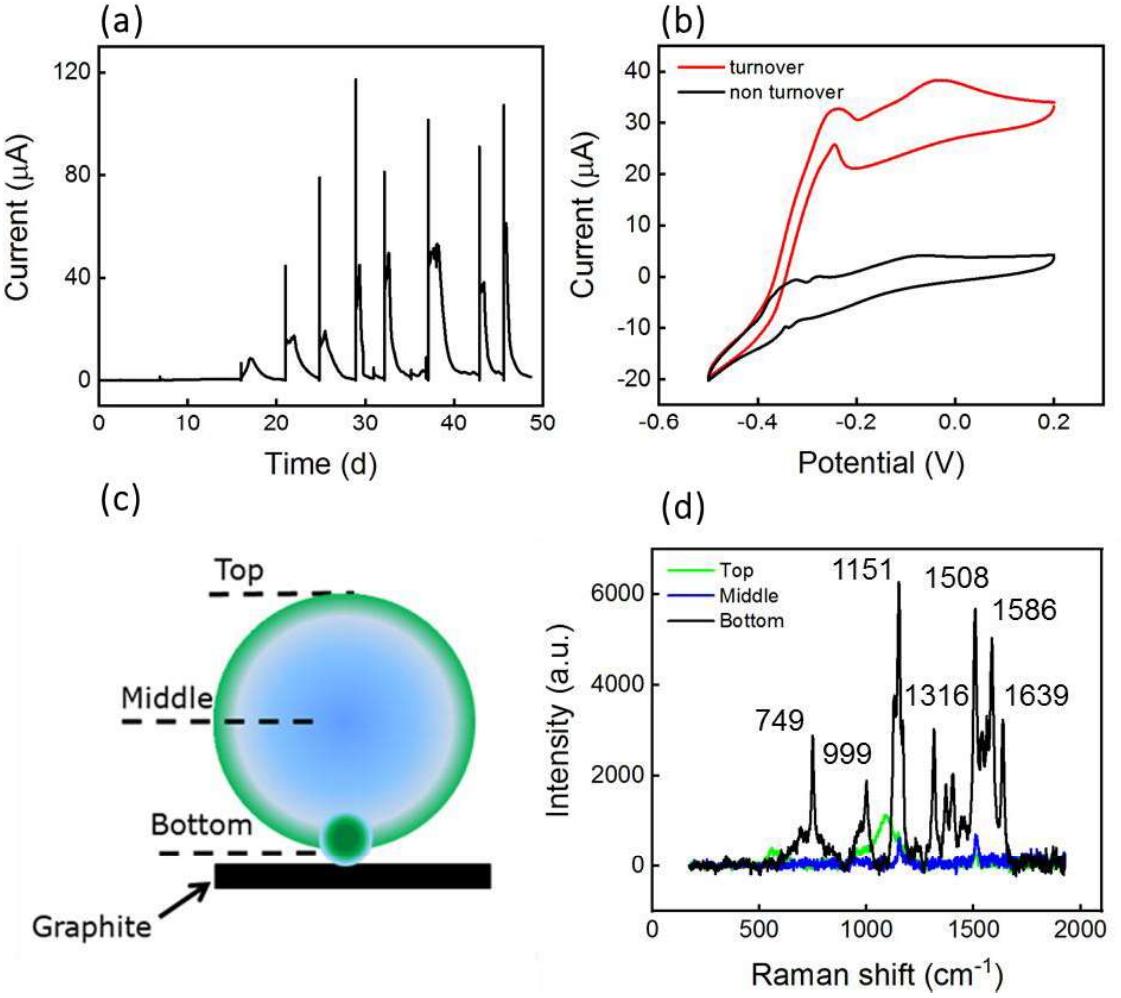

Figure 4. Electrochemical behavior of single EGS growing on the graphite. (a) CA, (b) CV profile and (c) sampling sites, (d) Raman spectrum. CA was performed at +0.2 V.

To gain insight into the mechanisms behind the capacitive behavior of the EGS bioanode, the electrochemical behavior of a single granule sludge was investigated. The setup for the test is shown in Figure S5. Single EGS was sedimented naturally on a graphite electrode (0.20 cm^2), and a 10 ml medium was refreshed to achieve an acetate concentration of 10 mM in each batch. Figure 4a shows the biocurrent generation from single EGS during the CA experiment, indicating the enrichment of electroactive bacteria. After 16 days, biocurrent generation increased gradually and reached a maximum level of 5.4 μA, and thereafter it declined due to the substrate exhaustion. After medium replacement, the biocurrent generation increased again. After several batches (approx. 37 days), a maximum current of approx. 50 μA was achieved. To elucidate the electron transfer mechanisms in the single EGS bioanode, CV at turnover (in the presence of electron donor) and non-turnover (acetate depletion) conditions were recorded. As shown in Figure 4b, a typical sigmoidal wave was observed for both conditions, demonstrating a good electroactivity of the EGS bioanode. However, the CV curve did not show straightforward information on the electron transfer site that was correlated with formal potential positions [36, 42]. Thus, the calculation of formal potential from the first derivative curve of CV was performed (Figure S6). In turnover CV, two major redox systems were distinguished, noted as redox system I at a formal potential of -0.344 V and system II at a formal potential of -0.275 V, respectively. Redox system I can be attributed to the direct electron transfer via outer membrane cytochromes like OmcB, OmcE and OmcS according to the potentials of membrane-bound electron transfer protein reported previously [43]. The positive shift of formal potential in the

second redox system may have resulted from a population of redox species whose current was not affected by diffusion [31].

In turnover conditions, when microorganisms were oxidizing substrates, multiple currents of each redox species were recorded in a CV curve and high catalytic current may overshadow the signals from individual redox species. Therefore, non-turnover CV analysis was performed to study the individual redox species related to interfacial electron transfer between redox centers [44]. Two redox peaks were obtained with the formal potential of -0.367 and -0.325 V. Both redox systems were associated with direct electron transfer which can be accommodated by the outer membrane cytochromes [29]. Particularly, the formal potential of -0.367 V was close to the formal potentials (-0.389 V) of c-type cytochromes expressed by *Geobacter sulfurreducens*, which points towards a *Geobacter* dominated biofilm. Thick biofilm was observed by the naked eye and reddish *Geobacter*-like bacteria were identified in the biofilm by microbial community analysis (Figure S7).

To further confirm this, Raman spectroscopy was performed on different sites (schematically described in Figure 4c) of the single EGS. As shown in Figure 4d, the spectrum of "Bottom" of single EGS shows typical characteristic features of c-type cytochromes [45-47], such as the main heme band at 1586 cm^{-1}, typical oxidation state-sensitive bands at 1316 with two additional minor bands at 1397 and 1406 cm^{-1}, and strong band at 1508 cm^{-1} (associated with heme interaction with a metallic surface) [46]. It has been reported that these characterized peaks were associated with the multi-heme of *G. sulfurreducens* cytochromes [47]. Additionally, the Raman absorption spectra also

showed multiple bands at 749, 999, 1151, and 1639 cm^{-1} with minor bands at 1228 cm^{-1}, which were assigned to the heme interaction with surrounding organic molecules [46]. The peak at 749 cm^{-1}could be from -O-H vibration of the periphery heme carboxylic group of the molecule [47], and the two main bands (1586 and 1639 cm^{-1}) were probably ascribed to the vibrations of the terapyrrole ring located at the center of heme which has been demonstrated to be sensitive to the heme oxidation state [46, 48]. Comparatively, no characterized peaks of cytochromes c were observed from the Raman spectra of "Top" and "Middle" sites of the single EGS. According to the above results, the cytochromes were well spatially structured according to formal potential and characterized Raman peaks. The cytochromes are not only involved in the respiratory electron transport chain, but also assisting in the electron transport [49] or transfer [50] via conductive nanowires. Thus, the results indicated that the out layer of EGS that was in good connection with the electrode might play an important role in effective electron flow between the single granule and graphite electrode. However, the electron flow mechanisms inside the granule remained unknown.

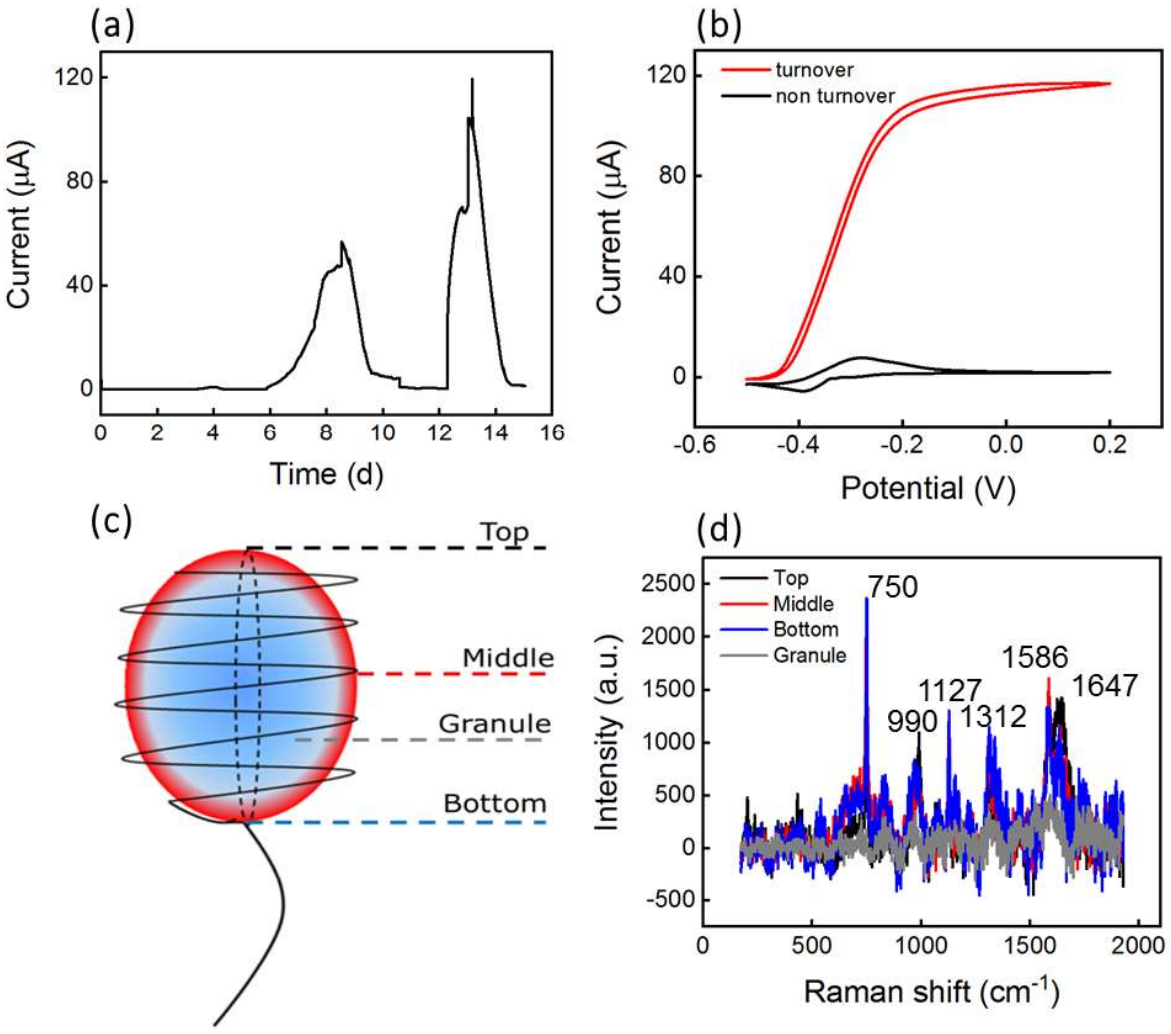

Figure 5. Electrochemical behavior of single EGS wrapped with gold wire. (a) CA, (b) CV profile and (c) sampling sites, (d) Raman spectrum. CA was performed at +0.2 V.

To further explore the importance of the direct connection between the out layer of EGS and electrode, the electrochemical behavior of single EGS wrapped by gold wire (Ø 0.1 mm, Figure 5c and Figure S8) was investigated by the similar CA (+0.2 V) and CV tests. CA profile showed a typical current generation in a fed-batch operation. At day 13 current reached a maximum level of 110 μA, and thereafter decreased due to the substrate

exhaustion. A rapid current response was immediately observed after replenishing medium, implying a good and stable electrochemical activity. The single granule, wrapped with gold wire, was analyzed by CV under turnover and non-turnover conditions (Figure 5b). The classic sigmoidal shape was observed for turnover CV, and formal potential of -0.322 V was obtained from its first derivative curve (Figure S9), indicating the strong association of outer membrane-cytochromes to electrocatalytic activity. Interestingly, at non-turnover conditions, microbes showed more complex behavior. From the derivative curve (Figure S9), it was observed that there was only one reduction inflection point, and three oxidation inflection points (represented by three single maximum in the curve) under non-catalytic conditions. The three oxidation peaks became distinguishable when the acetate was depleted. It could be due to that multiple redox species were involved in the electron transfer and exhibited different formal potentials or single redox mediator occupying different micro-environments [31]. Raman spectroscopy was performed on different sites of the single EGS. As expected, all the sampling sites (Top, Middle and Bottom), which were in good contact with gold wire, exhibited typical characterized peaks of cytochrome c (main heme bands at 1647 cm^{-1}, 1586 cm^{-1}, 1312 cm^{-1} and 750 cm^{-1}). Oppositely, in inner parts of the granule which were not in direct contact with gold wire, only noise peaks were observed. The results further verify that direct connection between single EGS and electrode may be favorable for the enrichment of electrogenic bacteria, which in return could promote the electron transfer through cytochrome c (as an electric conduit). Once the single EGS was moved from the gold wire, the biocurrent soon declined from 34.5 to 26.2 μA (Figure S10), which indicated

that they may also contribute to the current generation [51]. This result was in line with the previous multiple EGS experiment.

3.4. Microbial community dynamics under chronoamperometry

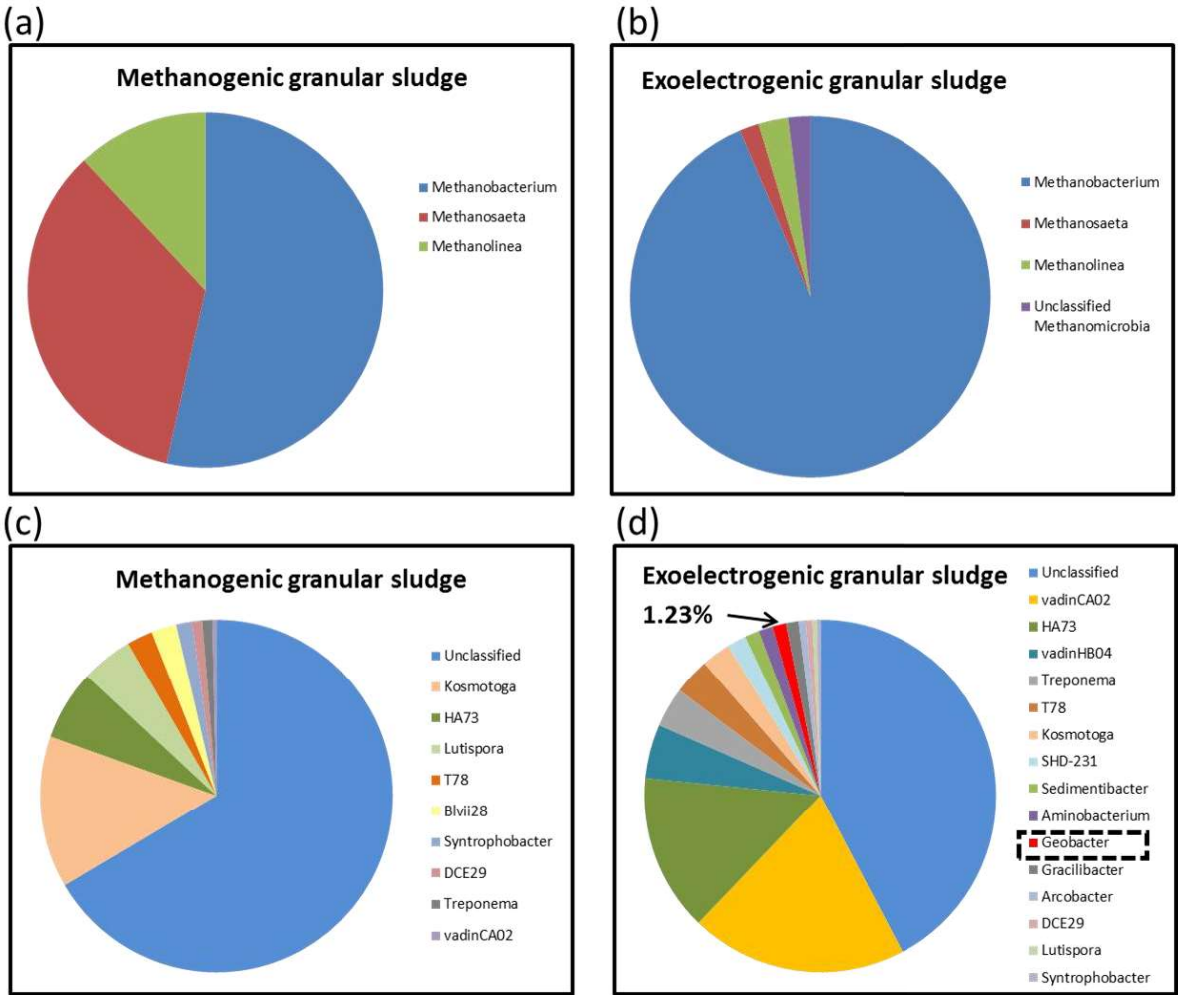

Figure 6. Taxonomic classification of the archaea and bacteria communities (over 0.1% of the relative abundance). The area of pie was based on the relative abundance, which was normalized by the relative abundance affiliated with the taxon divided by the total abundance of sequences per sample. (a) and (b) archaea-genus level; (c) and (d) bacteria-genus level.

It was hypothesized earlier that the superior capacitive performance of the EGS was most likely due to the enrichment of exoelectrogenic microorganisms. Therefore, disclosing the microbial community in the EGS and the methanogenic ones would be helpful for a better understanding of the electron storage process. Thus, microbial community dynamics were investigated under the CA program (anode potential at 0.02 V vs Ag/AgCl). The taxonomic classification of the archaeal communities at different levels is displayed in Figure 6a and 6c. The order level classification revealed that *Methanobacteriales* as hydrogenotrophic methanogens were dominant in methanogenic granular sludge and EGS samples, with a relative abundance of 53% and 93%, respectively. Besides, acetoclastic methanogens *Methanosarcinales* and hydrogenotrophic methanogens *Methanomicrobiales* were identified in both samples and decreased in cultivated EGS sample. The decrease in abundance of acetoclastic methanogens could be due to the inhibited methanogenic activity at positive anodic potential [52]. At the genus level, more than 93% of the sequences from EGS were assigned to *Methanobacterium*, while it only accounted for 53% in methanogenic granular sludge. Besides, *Methanosaeta*, which is known as a unique methanogen exclusively using acetate [53], decreased significantly at the end of the experiment (from 34% to 1%). The results suggested that the acetoclastic methanogens were seriously suppressed after elevating anodic potential indicating their higher sensitivity to the increased redox potential.

The taxonomic classification of the bacterial communities is depicted in Figure 6b and 6d. The phylum-level classification showed that *Firmicutes* (26%), *Bacteroidetes* (17%), *Thermotogae* (14%), *Proteobacteria* (11%), followed by *Synergistetes* (8%), *Tenericutes*

(7%) and others (17%) were the most dominant bacteria in methanogenic granular sludge. Comparatively, in the EGS, the microbial community composition changed and was mainly dominated by *Synergistetes* (36%), *Bacteroidetes* (32%), *Firmicutes* (15%), followed by *Chloroflexi* (7%), *Proteobacteria* (3%) and others (7%). The *Proteobacteria*, *Synergistetes*, *Firmicutes* and *Bacteroidetes* were often found in the electroactive anode [54, 55]. The different phyla distribution suggested that the granular sludge community was greatly changed after the proliferation of exoelectrogens at the positive anodic potential. At the order level, in methanogenic granular sludge, *Bacteroidales* (17%), *Thermotogales* (14%), followed by *Campylobacterales* (10%) were the most abundant, whereas, in exoelectrogenic granular sludge, *Synergistales* (36%), *Bacteroidales* (17%), followed by *Clostridiales* (12%) were predominant. Interestingly, *Desulfuromonadales* was present after the successful transformation of granular sludge from methanogenic to exoelectrogenic conditions. Many species belonging to *Desulfuromonadales* have been reported as electroactive bacteria [56]. The genus-level classification confirmed that the *Desulfuromonadales* was affiliated with genus *Geobacter* (relative abundance of 1.2%), which was known for its ability for direct extracellular electrons transfer via conductive nanowire [57-59]. The above results further confirmed the enrichment of exoelectrogens in granular sludge, which in turn indicated the role of exoelectrogens in granular sludge for electron storage.

(Proposed mechanism of charge storage in EGS) In light of the results above, a potential mechanism of charge storage in the biocapacitor was proposed. When the organic matter was oxidized by exoelectrogens, the electrons are released and stored in the c-type cytochromes or nanowires [60]. Thereafter, some of the electrons were transferred to the

outer membrane of cells, which may induce the adsorption of the cation ions on the surface of granule sludge and thereby forming a typical electrical double layer (similar to activated carbon granule) [11]. Besides, the cytochrome c as a redox cofactor itself can also store the charge generated from organics oxidation.

The potential contributions of cytochromes and electrical double layer to the electron storage were proved in this study, but it still remains unclear which of them was the most dominant mechanism. There are several approaches to clarify this. For example, detection of the cytochromes in EGS using proteomics or RNA analysis could gain a better understanding of the functional role of c-type cytochromes. Besides, the effect of the electrical double layer could be demonstrated by adding suitable reagents (i.e. ethylenediaminetetraacetic acid) to remove/exclude the cations in the electrolyte.

3.5. Significance and perspectives

The present work for the first time reported an EGS-based biocapacitor for electron extracting and accumulation from wastewater. Compared to the other abiotic materials such as activated carbon granule-based biocapacitors, the EGS-based biocapacitor has its own merits. Firstly, the dense exoelectrogens and innate 3D granular structure enable a good capacity of electron storage in the EGS-based bioanode. Secondly, the EGS was much cheaper than the activated carbon granule (as stated in Introduction). Lastly, the amount of electron storage in 20 g EGS (1542.7 ± 203.2 mC) was higher than the maximum value reported so far (860 mC, single activater granule) [11].

Though promising, more efforts should be made to find a suitable niche for its real application. First of all, considering the complex pH range of real wastewater, the biocapacitor performance under different pH conditions should be investigated to better

understand the applicable pH range. Secondly, the capacitive current could be advantageous when using EGS granules in fluidized microbial fuel cell reactors, where charging EGS in one stage/chamber, and discharging in another stage/chamber as described earlier [61]. Thirdly, to improve the overall capacitive performance of the novel biocapacitor, a good contact among EGS granules and current collector was of utmost importance. In that case, the low internal resistance would, in turn, boost the electron flow. When the maximum capacitance is achieved in an ideal case, there will be several potential applications such as to power sensors, lighting, pumps or robots which consume pulsed current/power [39].

4. Conclusions

This proof-of-concept study successfully demonstrated, both in multiple and single granular sludge level, the capacitive capability of the EGS. Such a novel biocapacitor based on EGS not only can extract the chemical energy from organic waste streams but also can take its unique advantages of the granular structure and capacitive c-type cytochromes to store electric charges. With the EGS, 1542.7 ± 203.2 mC charge was harvested and stored from synthetic wastewater, when it was charged for 5 minutes at +0.2 V vs Ag/AgCl and discharged for 10 minutes. The charge could be potentially applied to power small devices with low energy demand, i.e. biosensors. Thus, we envisage the EGS-based biocapacitor to be a promising and alternative electron storage device, which will open an avenue towards a cheap, renewable and carbon-neutral biocapacitor.

Credit Author Statement

Nannan Zhao: Investigation, Methodology, Validation, Formal analysis, Writing - original draft. Yanyan Su: Writing - review & editing. Irini Angelidaki: Supervision, Validation, Funding acquisition. Yifeng Zhang: Conceptualization, Supervision, Funding acquisition.

Acknowledgements

This work was supported by China Scholarship Council, EliteForsk travel funding offered by Danish Ministry of Education and Research. Nannan Zhao thanks Huan Liang for constructive discussion on electronics, Alexksandra Kulagowska and Colsen (The Netherlands) for providing anaerobic granular sludge.

Competing interests

The authors declare no competing interests.

References

[1]. Zhou, Y. J.,Kerkhoven, E. J., and Nielsen, J., 2018. Barriers and opportunities in bio-based production of hydrocarbons. *Nat Energy*. DOI: 10.1038/s41560-018-0197-x.

[2]. Lovley, D. R., 2006. Bug juice: harvesting electricity with microorganisms (vol 4, pg 497, 2006). *Nat Rev Microbiol 4*, (10), 797-797. DOI: 10.1038/nrmicro1442.

[3]. Saar, K. L.,Bombelli, P.,Lea-Smith, D. J.,Call, T.,Aro, E.-M.,Müller, T.,Howe, C. J., and Knowles, T. P. J., 2018. Enhancing power density of biophotovoltaics by decoupling storage and power delivery. *Nat Energy 3*, (1), 75-81. DOI: 10.1038/s41560-017-0073-0.

[4]. Zeng, Z.,Murugesan, V.,Han, K. S.,Jiang, X.,Cao, Y.,Xiao, L.,Ai, X.,Yang, H.,Zhang, J.-G.,Sushko, M. L., and Liu, J., 2018. Non-flammable electrolytes with high

salt-to-solvent ratios for Li-ion and Li-metal batteries. *Nat Energy 3*, (8), 674-681. DOI: 10.1038/s41560-018-0196-y.

[5]. Kumar, A.,Hsu, L. H. H.,Kavanagh, P.,Barriere, F.,Lens, P. N. L.,Lapinsonniere, L.,Lienhard, J. H.,Schroder, U.,Jiang, X. C., and Leech, D., 2017. The ins and outs of microorganism-electrode electron transfer reactions. *Nat Rev Chem 1*, (3). DOI: 10.1038/s41570-017-0024.

[6]. Sawatdeenarunat, C.,Surendra, K. C.,Takara, D.,Oechsner, H., and Khanal, S. K., 2015. Anaerobic digestion of lignocellulosic biomass: Challenges and opportunities. *Bioresour Technol 178*, 178-186. DOI: https://doi.org/10.1016/j.biortech.2014.09.103.

[7]. Miller, J. R. And Simon, P., 2008. Materials science - Electrochemical capacitors for energy management. *Science 321*, (5889), 651-652. DOI: 10.1126/science.1158736.

[8]. Simon, P. and Gogotsi, Y., 2008. Materials for electrochemical capacitors. *Nat Mater 7*, (11), 845-854. DOI: 10.1038/nmat2297.

[9]. Logan, B. E. and Rabaey, K., 2012. Conversion of Wastes into Bioelectricity and Chemicals by Using Microbial Electrochemical Technologies. *Science 337*, (6095), 686-690. DOI: 10.1126/science.1217412.

[10]. Deeke, A.,Sleutels, T. H.,Hamelers, H. V., and Buisman, C. J., 2012. Capacitive bioanodes enable renewable energy storage in microbial fuel cells. *Environ Sci Technol 46*, (6), 3554-60. DOI: 10.1021/es204126r.

[11]. Borsje, C.,Liu, D. D.,Sleutels, T.,Buisman, C. J. N., and ter Heijne, A., 2016. Performance of single carbon granules as perspective for larger scale capacitive bioanodes. *J Power Sources 325*, 690-696. DOI: 10.1016/j.jpowsour.2016.06.092.

[12]. Ren, H.,Tian, H.,Lee, H. S.,Park, T.,Leung, F. C.,Ren, T. L., and Chae, J., 2015. Regulating the respiration of microbe: A bio-inspired high performance microbial supercapacitor with graphene based electrodes and its kinetic features. *Nano Energy 15*, 697-708. DOI: 10.1016/j.nanoen.2015.05.030.

[13]. Malvankar, N. S.,Mester, T.,Tuominen, M. T., and Lovley, D. R., 2012. Supercapacitors based on c-type cytochromes using conductive nanostructured networks of living bacteria. *Chemphyschem 13*, (2), 463-8. DOI: 10.1002/cphc.201100865.

[14]. Schmidt, J. E. and Ahring, B. K., 1996. Granular sludge formation in upflow anaerobic sledge blanket (UASB) reactors. *Biotechnol Bioeng 49*, (3), 229-246. DOI: 10.1002/(sici)1097-0290(19960205)49:3<229::aid-bit1>3.0.co;2-m.

[15]. Morita, M.,Malvankar, N. S.,Franks, A. E.,Summers, Z. M.,Giloteaux, L.,Rotaru, A. E.,Rotaru, C., and Lovley, D. R., 2011. Potential for Direct Interspecies Electron Transfer in Methanogenic Wastewater Digester Aggregates. *Mbio 2*, (4), 1-8. DOI: 10.1128/mBio.00159-11.

[16]. Lovley, D. R., 2017. Happy together: microbial communities that hook up to swap electrons. *Isme Journal 11*, (2), 327-336. DOI: 10.1038/ismej.2016.136.

[17]. Kim, J. R.,Min, B., and Logan, B. E., 2005. Evaluation of procedures to acclimate a microbial fuel cell for electricity production. *Appl Microbiol Biotechnol 68*, (1), 23-30. DOI: 10.1007/s00253-004-1845-6.

[18]. Balch, W. E.,Fox, G. E.,Magrum, L. J.,Woese, C. R., and Wolfe, R. S., 1979. Methanogens-Re-Evaluation of a unique biological group. *Microbiol Rev 43*, (2), 260-296, <Go to ISI>://WOS:A1979HC66200006.

[19]. Zhao, N.,Treu, L.,Angelidaki, I., and Zhang, Y., 2019. Exoelectrogenic Anaerobic Granular Sludge for Simultaneous Electricity Generation and Wastewater Treatment. *Environ Sci Technol* *53*, (20), 12130-12140. DOI: 10.1021/acs.est.9b03395.

[20]. Leong, J. X.,Daud, W. R. W.,Ghasemi, M.,Ben Liew, K., and Ismail, M., 2013. Ion exchange membranes as separators in microbial fuel cells for bioenergy conversion: A comprehensive review. *Renew Sust Energ Rev.* *28*, 575-587. DOI: 10.1016/j.rser.2013.08.052.

[21]. Zhao, N.,Jiang, Y.,Alvarado-Morales, M.,Treu, L.,Angelidaki, I., and Zhang, Y., 2018. Electricity generation and microbial communities in microbial fuel cell powered by macroalgal biomass. *Bioelectrochemistry* *123*, 145-149. DOI: 10.1016/j.bioelechem.2018.05.002.

[22]. Frackowiak, E. and Beguin, F., 2001. Carbon materials for the electrochemical storage of energy in capacitors. *Carbon* *39*, (6), 937-950. DOI: 10.1016/s0008-6223(00)00183-4.

[23]. Bellouti, M.,Alves, M. M.,Novais, J. M., and Mota, M., 1997. Flocs vs granules: Differentiation by fractal dimension. *Water Res* *31*, (5), 1227-1231. DOI: 10.1016/s0043-1354(96)00347-8.

[24]. Quarmby, J. and Forster, C. F., 1995. A comparative study of the internal architecture of anaerobic granular sludges. *J Chem Technol Biotechnol* *63*, (1), 60-68. DOI: 10.1002/jctb.280630109.

[25]. Torres, C. I.,Krajmalnik-Brown, R.,Parameswaran, P.,Marcus, A. K.,Wanger, G.,Gorby, Y. A., and Rittmann, B. E., 2009. Selecting Anode-Respiring Bacteria Based

on Anode Potential: Phylogenetic, Electrochemical, and Microscopic Characterization. *Environ Sci Technol 43*, (24), 9519-9524. DOI: 10.1021/es902165y.

[26]. Sevda, S.,Dominguez-Benetton, X.,Vanbroekhoven, K.,Sreekrishnan, T. R., and Pant, D., 2013. Characterization and comparison of the performance of two different separator types in air–cathode microbial fuel cell treating synthetic wastewater. *Chem Eng J 228*, 1-11. DOI: 10.1016/j.cej.2013.05.014.

[27]. Satoh, H.,Miura, Y.,Tsushima, I., and Okabe, S., 2007. Layered structure of bacterial and archaeal communities and their in situ activities in anaerobic granules. *Appl Environ Microbiol 73*, (22), 7300-7307. DOI: 10.1128/AEM.01426-07.

[28]. Bond, D. R. and Lovley, D. R., 2003. Electricity Production by Geobacter sulfurreducens Attached to Electrodes. *Appl Environ Microbiol 69*, (3), 1548-1555. DOI: 10.1128/aem.69.3.1548-1555.2003.

[29]. Fricke, K.,Harnisch, F., and Schröder, U., 2008. On the use of cyclic voltammetry for the study of anodic electron transfer in microbial fuel cells. *Energy Environ Sci 1*, (1), 144. DOI: 10.1039/b802363h.

[30]. Du, Q.,Li, T.,Li, N., and Wang, X., 2017. Protection of Electroactive Biofilm from Extreme Acid Shock by Polydopamine Encapsulation. *Environ Sci Technol Letters 4*, (8), 345-349. DOI: 10.1021/acs.estlett.7b00242.

[31]. Strycharz, S. M.,Malanoski, A. P.,Snider, R. M.,Yi, H.,Lovley, D. R., and Tender, L. M., 2011. Application of cyclic voltammetry to investigate enhanced catalytic current generation by biofilm-modified anodes of Geobacter sulfurreducens strain DL1 vs. variant strain KN400. *Energy Environ Sci 4*, (3), 896-913. DOI: 10.1039/c0ee00260g.

[32]. Bonanni, P. S.,Schrott, G. D.,Robuschi, L., and Busalmen, J. P., 2012. Charge accumulation and electron transfer kinetics in Geobacter sulfurreducens biofilms. *Energy Environ Sci 5*, (3), 6188. DOI: 10.1039/c2ee02672d.

[33]. Zhang, X.,He, W.,Ren, L.,Stager, J.,Evans, P. J., and Logan, B. E., 2015. COD removal characteristics in air-cathode microbial fuel cells. *Bioresour Technol 176*, 23-31. DOI: 10.1016/j.biortech.2014.11.001.

[34]. Strycharz-Glaven, S. M.,Snider, R. M.,Guiseppi-Elie, A., and Tender, L. M., 2011. On the electrical conductivity of microbial nanowires and biofilms. *Energy Environ Sci 4*, (11), 4366. DOI: 10.1039/c1ee01753e.

[35]. Jadhav, D. A.,Chendake, A. D.,Schievano, A., and Pant, D., 2019. Suppressing methanogens and enriching electrogens in bioelectrochemical systems. *Bioresour Technol 277*, 148-156. DOI: https://doi.org/10.1016/j.biortech.2018.12.098.

[36]. Carmona-Martinez, A. A.,Harnisch, F.,Kuhlicke, U.,Neu, T. R., and Schroder, U., 2013. Electron transfer and biofilm formation of Shewanella putrefaciens as function of anode potential. *Bioelectrochemistry 93*, 23-9. DOI: 10.1016/j.bioelechem.2012.05.002.

[37]. Schroder, U., 2007. Anodic electron transfer mechanisms in microbial fuel cells and their energy efficiency. *Phys Chem Chem Phys 9*, (21), 2619-29. DOI: 10.1039/b703627m.

[38]. Grebenko, A.,Dremov, V.,Barzilovich, P.,Bubis, A.,Sidoruk, K.,Voeikova, T.,Gagkaeva, Z.,Chernov, T.,Korostylev, E.,Gorshunov, B., and Motovilov, K., 2018. Impedance spectroscopy of single bacterial nanofilament reveals water-mediated charge transfer. *PLoS One 13*, (1), e0191289. DOI: 10.1371/journal.pone.0191289.

[39]. Caizan-Juanarena, L.,Borsje, C.,Sleutels, T.,Yntema, D.,Santoro, C.,Ieropoulos, I.,Soavi, F., and Ter Heijne, A., 2020. Combination of bioelectrochemical systems and electrochemical capacitors: Principles, analysis and opportunities. *Biotechnol Adv* *39*, 107456. DOI: 10.1016/j.biotechadv.2019.107456.

[40]. Lu, Z.,Girguis, P.,Liang, P.,Shi, H.,Huang, G.,Cai, L., and Zhang, L., 2015. Biological capacitance studies of anodes in microbial fuel cells using electrochemical impedance spectroscopy. *Bioprocess Biosyst Eng* *38*, (7), 1325-33. DOI: 10.1007/s00449-015-1373-z.

[41]. Wang, G.,Zhang, L., and Zhang, J., 2012. A review of electrode materials for electrochemical supercapacitors. *Chem Soc Rev* *41*, (2), 797-828. DOI: 10.1039/c1cs15060j.

[42]. Carmona-Martinez, A. A.,Harnisch, F.,Fitzgerald, L. A.,Biffinger, J. C.,Ringeisen, B. R., and Schroder, U., 2011. Cyclic voltammetric analysis of the electron transfer of Shewanella oneidensis MR-1 and nanofilament and cytochrome knock-out mutants. *Bioelectrochemistry* *81*, (2), 74-80. DOI: 10.1016/j.bioelechem.2011.02.006.

[43]. Stephen, C. S.,LaBelle, E. V.,Brantley, S. L., and Bond, D. R., 2014. Abundance of the multiheme c-type cytochrome OmcB increases in outer biofilm layers of electrode-grown Geobacter sulfurreducens. *PLoS One* *9*, (8), e104336. DOI: 10.1371/journal.pone.0104336.

[44]. Marsili, E.,Sun, J., and Bond, D. R., 2010. Voltammetry and Growth Physiology of Geobacter sulfurreducens Biofilms as a Function of Growth Stage and Imposed Electrode Potential. *Electroanalysis* *22*, (7-8), 865-874. DOI: 10.1002/elan.200800007.

[45]. Hu, S.,Morris, I. K.,Singh, J. P.,Smith, K. M., and Spiro, T. G., 1993. Complete assignment of cytochrome c resonance Raman spectra via enzymic reconstitution with isotopically labeled hemes. *J Am Chem Soc 115*, (26), 12446-12458. DOI: 10.1021/ja00079a028.

[46]. Dick, L. A.,Haes, A. J., and Van Duyne, R. P., 2000. Distance and Orientation Dependence of Heterogeneous Electron Transfer: A Surface-Enhanced Resonance Raman Scattering Study of Cytochrome c Bound to Carboxylic Acid Terminated Alkanethiols Adsorbed on Silver Electrodes. *J Phy Chem B 104*, (49), 11752-11762. DOI: 10.1021/jp0029717.

[47]. Lebedev, N.,Strycharz-Glaven, S. M., and Tender, L. M., 2014. Spatially resolved confocal resonant Raman microscopic analysis of anode-grown Geobacter sulfurreducens biofilms. *Chemphyschem 15*, (2), 320-7. DOI: 10.1002/cphc.201300984.

[48]. Murgida, D. H. and Hildebrandt, P., 2008. Disentangling interfacial redox processes of proteins by SERR spectroscopy. *Chem Soc Rev 37*, (5), 937-45. DOI: 10.1039/b705976k.

[49]. Gorby, Y. A.,Yanina, S.,McLean, J. S.,Rosso, K. M.,Moyles, D.,Dohnalkova, A.,Beveridge, T. J.,Chang, I. S.,Kim, B. H.,Kim, K. S.,Culley, D. E.,Reed, S. B.,Romine, M. F.,Saffarini, D. A.,Hill, E. A.,Shi, L.,Elias, D. A.,Kennedy, D. W.,Pinchuk, G.,Watanabe, K.,Ishii, S.,Logan, B.,Nealson, K. H., and Fredrickson, J. K., 2006. Electrically conductive bacterial nanowires produced by Shewanella oneidensis strain MR-1 and other microorganisms. *Proc Natl Acad Sci U S A 103*, (30), 11358-63. DOI: 10.1073/pnas.0604517103.

[50]. Inoue, K.,Leang, C.,Franks, A. E.,Woodard, T. L.,Nevin, K. P., and Lovley, D. R., 2011. Specific localization of the c-type cytochrome OmcZ at the anode surface in current-producing biofilms of Geobacter sulfurreducens. *Environ Microbiol Rep* *3*, (2), 211-7. DOI: 10.1111/j.1758-2229.2010.00210.x.

[51]. Du, Q.,Mu, Q.,Cheng, T.,Li, N., and Wang, X., 2018. Real-Time Imaging Revealed That Exoelectrogens from Wastewater Are Selected at the Center of a Gradient Electric Field. *Environ Sci Technol* *52*, (15), 8939-8946. DOI: 10.1021/acs.est.8b01468.

[52]. He, Z.,Minteer, S. D., and Angenent, L. T., 2005. Electricity generation from artificial wastewater using an upflow microbial fuel cell. *Environ Sci Technol* *39*, (14), 5262-5267. DOI: 10.1021/es0502876.

[53]. Zhang, Y. and Angelidaki, I., 2012. A simple and rapid method for monitoring dissolved oxygen in water with a submersible microbial fuel cell (SBMFC). *Biosens Bioelectron* *38*, (1), 189-94. DOI: 10.1016/j.bios.2012.05.032.

[54]. Lesnik, K. L. and Liu, H., 2014. Establishing a core microbiome in acetate-fed microbial fuel cells. *Appl Microbiol Biotechnol* *98*, (9), 4187-96. DOI: 10.1007/s00253-013-5502-9.

[55]. Zhi, W.,Ge, Z.,He, Z., and Zhang, H., 2014. Methods for understanding microbial community structures and functions in microbial fuel cells: a review. *Bioresour Technol* *171*, 461-8. DOI: 10.1016/j.biortech.2014.08.096.

[56]. Takahashi, S.,Miyahara, M.,Kouzuma, A., and Watanabe, K., 2016. Electricity generation from rice bran in microbial fuel cells. *Bioresour Bioprocess* *3*, (1), 50. DOI: 10.1186/s40643-016-0129-1.

[57]. Reguera, G.,McCarthy, K. D.,Mehta, T.,Nicoll, J. S.,Tuominen, M. T., and Lovley, D. R., 2005. Extracellular electron transfer via microbial nanowires. *Nature 435*, 1098. DOI: 10.1038/nature03661 https://www.nature.com/articles/nature03661#supplementary-information.

[58]. Adhikari, R. Y.,Malvankar, N. S.,Tuominen, M. T., and Lovley, D. R., 2016. Conductivity of individual Geobacter pili. *RSC Advances 6*, (10), 8354-8357. DOI: 10.1039/c5ra28092c.

[59]. Reguera, G.,Pollina, R. B.,Nicoll, J. S., and Lovley, D. R., 2007. Possible nonconductive role of Geobacter sulfurreducens pilus nanowires in biofilm formation. *J Bacteriol 189*, (5), 2125-2127. DOI: 10.1128/jb.01284-06.

[60]. Wang, F.,Gu, Y.,O'Brien, J. P.,Yi, S. M.,Yalcin, S. E.,Srikanth, V.,Shen, C.,Vu, D.,Ing, N. L.,Hochbaum, A. I.,Egelman, E. H., and Malvankar, N. S., 2019. Structure of Microbial Nanowires Reveals Stacked Hemes that Transport Electrons over Micrometers. *Cell 177*, (2), 361-369.e10. DOI: https://doi.org/10.1016/j.cell.2019.03.029.

[61]. Deeke, A.,Sleutels, T. H. J. A.,Donkers, T. F. W.,Hamelers, H. V. M.,Buisman, C. J. N., and Ter Heijne, A., 2015. Fluidized Capacitive Bioanode As a Novel Reactor Concept for the Microbial Fuel Cell. *Environ Sci Technol 49*, (3), 1929-1935. DOI: 10.1021/es503063n.

Supplementary Materials

Click here to download Supplementary Materials: Supplementary materials.docx

***Credit Author Statement**

Credit Author Statement

Nannan Zhao: Investigation, Methodology, Validation, Formal analysis, Writing - original draft. **Yanyan Su**: Writing - review & editing. **Irini Angelidaki**: Supervision, Validation, Funding acquisition. **Yifeng Zhang**: Conceptualization, Supervision, Funding acquisition.

***Declaration of Interest Statement**

Declaration of interests

☒ The authors declare that they have no known competing financial interests or personal relationships that could have appeared to influence the work reported in this paper.

☐The authors declare the following financial interests/personal relationships which may be considered as potential competing interests: